Magnetostatic Volume Modes of Ferrite Thin Films with Magnetization Inhomogeneities Through the Film Thickness

NIKOLAOS E. BURIS, STUDENT MEMBER, IEEE, AND DANIEL D. STANCIL, MEMBER, IEEE

Abstract —**A variational method recently used to analyze magnetostatic surface waves in films with arbitrary magnetization inhomogeneities through the film thickness is extended and applied to volume-wave modes in similar structures. Methods for calculating dispersion relations, delay characteristics, and magnetostatic potential functions for both forward and backward volume waves are discussed. Also, concepts pertaining to homogeneous films such as mode bandwidth and dimensional scaling effects are extended to the inhomogeneous case. Detailed consideration is given to a class of modes whose zero-wavenumber cutoff frequencies are associated with the minimum magnetization of the film. Calculations for linear and ion-implanted films are presented as numerical examples. Forward volume waves show greater sensitivity to the inhomogeneities than do backward volume waves for the cases considered.**

I. Introduction

In a PREVIOUS paper [1], we used a variational approach to solve the problem of magnetostatic surface-wave (MSSW) propagation in ferrite thin films with nonuniform magnetization through the film thickness. The geometry considered consisted of an infinite slab placed between parallel ground planes. In the present paper, we discuss the propagation of volume magnetostatic waves in these inhomogeneous films.

In contrast to surface waves, the properties of both backward volume-wave (BVW) as well as forward volume-wave (FVW) modes are independent of the direction of propagation in this geometry despite the magnetization inhomogeneities [2].

As in the surface-wave case, the problem will be solved by employing a variational principle approach to the boundary value problem. The potential in the ferrimagnetic region is expanded in a complete set of functions, and the expansion coefficients are found by Ritz' method.

Linear magnetization profiles are used for illustration of the method and the effect of the slope of their magnetization is presented. Magnetization profiles resulting from low-level ion implantation of ferrimagnetic films are also presented, and the effect of the implantation level on the magnetostatic-wave (MSW) delay is discussed.

Manuscript received February 20, 1985; revised May 13, 1985. This work was supported in part by the Rome Air Development Center Electromagnetic Sciences Division, Hanscom Air Force Base, MA.

The authors are with the Electrical and Computer Engineering Department, North Carolina State University, Raleigh, NC 27695-7911.

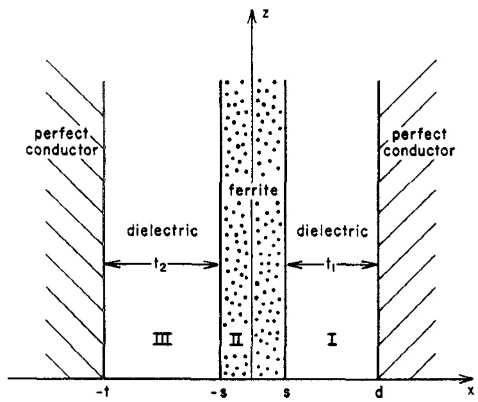

Fig. 1. Ferrite film geometry and coordinate system used.

II. Film Geometry and Basic Equations

Let us assume an infinite ferrite slab of thickness $2s$ placed between two infinite parallel perfect conductors as shown in Fig. 1. Consider a coordinate system with its origin at the middle of the slab with the z-axis parallel to the slab and the conductors.

Magnetostatic volume waves propagate in film structures under two different orientations of the bias field. BVW's propagate along the z-direction when the ferrimagnet is saturated with a bias field $\overline{H} = H_0\hat{z}$, while FVW's propagate along the z-direction when the bias field is normal to the plane of the film, i.e., $\overline{H} = H_0\hat{x}$.

With a small-signal time dependence of the form $e^{-i\omega t}$, the permeability tensor of the ferrimagnetic material takes the form

$$\bar{\bar{\mu}} = \mu_0 \begin{bmatrix} \mu & -i\kappa & 0 \\ i\kappa & \mu & 0 \\ 0 & 0 & 1 \end{bmatrix} \tag{1}$$

for BVW (bias $\overline{H} = H_0\hat{z}$), and the form

$$\bar{\bar{\mu}} = \mu_0 \begin{bmatrix} 1 & 0 & 0 \\ 0 & \mu & -i\kappa \\ 0 & i\kappa & \mu \end{bmatrix} \tag{2}$$

0018-9480/85/1000-1089$01.00 ©1985 IEEE

for FVW (bias $\bar{H} = H_0\hat{x}$), where

$$\mu = \frac{\gamma^2\mu_0^2 H_i(H_i + M_s) - \omega^2}{\gamma^2\mu_0^2 H_i^2 - \omega^2} \tag{3}$$

$$\kappa = \frac{-\gamma\mu_0 M_s\omega}{\gamma^2\mu_0^2 H_i^2 - \omega^2} \tag{4}$$

γ is the gyromagnetic ratio (negative), μ_0 is the permeability of free space, $M_s(x)$ is the saturation magnetization of the film as a function of position, and H_i is the internal magnetic field in the ferrimagnetic film.

Consistent with the magnetostatic approximation, we assume that there exists a potential function ψ such that

$$\bar{h} = -\nabla\psi \tag{5}$$

and

$$\bar{b} = \bar{\bar{\mu}}\cdot\bar{h}. \tag{6}$$

The equation that determines the potential ψ is Maxwell's equation requiring the divergence of the $\bar{b}$ field to vanish

$$\nabla\cdot(\bar{\bar{\mu}}\cdot\nabla\psi) = 0. \tag{7}$$

The boundary conditions to be satisfied are

$$\bar{b}\cdot\hat{x} \quad \text{continuous} \tag{8}$$

and

$$\psi \quad \text{continuous.} \tag{9}$$

Equation (7) reduces to Laplace's equation in the dielectric regions where M_s vanishes. The general solutions of (7) that represent waves traveling along the z-direction are of the form

$$\psi_{\mathrm{I}} = (A_1 e^{-\beta x} + A_2 e^{\beta x})e^{i\beta z} \tag{10a}$$

$$\psi_{\mathrm{II}} = \Phi(x)e^{i\beta z} \tag{10b}$$

$$\psi_{\mathrm{III}} = (D_1 e^{-\beta x} + D_2 e^{\beta x})e^{i\beta z}. \tag{10c}$$

Substitution of (10) into (5) gives the following expression for the small-signal field $\bar{h}$:

$$\bar{h}_{\mathrm{I}} = \left[\beta(A_1 e^{-\beta x} - A_2 e^{\beta x})\hat{x} - i\beta(A_1 e^{-\beta x} + A_2 e^{\beta x})\hat{z}\right]e^{i\beta z} \tag{11a}$$

$$\bar{h}_{\mathrm{II}} = -\left[\Phi'(x)\hat{x} + i\beta\Phi(x)\hat{z}\right]e^{i\beta z} \tag{11b}$$

$$\bar{h}_{\mathrm{III}} = \left[\beta(D_1 e^{-\beta x} - D_2 e^{\beta x})\hat{x} - i\beta(D_1 e^{-\beta x} + D_2 e^{\beta x})\hat{z}\right]e^{i\beta z}. \tag{11c}$$

III. Variational Formulation for BVW

Since the bias field is in-plane for BVW's, the internal field H_i is equal to the applied field H_o. Using the expression (1) for the permeability tensor, (6) yields for the $\bar{b}$ field

$$\bar{b}_{\mathrm{I}} = \mu_0\bar{h}_{\mathrm{I}} \tag{12a}$$

$$\bar{b}_{\mathrm{II}} = -\mu_0\left[\mu\Phi'\hat{x} + i\kappa\Phi'\hat{y} + i\beta\Phi\hat{z}\right]e^{i\beta z} \tag{12b}$$

$$\bar{b}_{\mathrm{III}} = \mu_0\bar{h}_{\mathrm{III}}. \tag{12c}$$

Requiring the divergence of (12b) to vanish (cf. eq. (7)) gives the equation

$$\mu\Phi'' + \mu'\Phi' - \beta^2\Phi = 0 \tag{13}$$

for the potential profile $\Phi(x)$ inside the ferrimagnet.

Application of the boundary condition (8) on the conductors and on the ferrimagnet–dielectric interfaces gives

$$A_1 e^{-\beta d} - A_2 e^{\beta d} = 0 \tag{14}$$

$$D_1 e^{\beta t} - D_2 e^{-\beta t} = 0 \tag{15}$$

$$-\mu\Phi'|_s = \beta(A_1 e^{-\beta s} - A_2 e^{\beta s}) \tag{16}$$

$$-\mu\Phi'|_{-s} = \beta(D_1 e^{\beta s} - D_2 e^{-\beta s}) \tag{17}$$

while the application of condition (9) at the interfaces gives

$$A_1 e^{-\beta s} + A_2 e^{\beta s} = \Phi(s) \tag{18}$$

$$D_1 e^{\beta s} + D_2 e^{-\beta s} = \Phi(-s). \tag{19}$$

Equation (13) cannot be solved analytically in closed form for the general case where μ is a function of x. For a numerical solution, we will formulate the boundary value problem as an equivalent variational one, noting that (13) can be obtained as the Euler–Lagrange derivative of the Lagrangian

$$L = \mu(\Phi')^2 + \beta^2\Phi^2. \tag{20}$$

We therefore consider the functional

$$w = \mu_0\int_{-s}^{s}\left[\mu(\Phi')^2 + \beta^2\Phi^2\right]dx + \mu_0 F_1(\Phi)|_s + \mu_0 F_2(\Phi)|_{-s} \tag{21}$$

where $F_1(\Phi)$ and $F_2(\Phi)$ are functions to be chosen so as to satisfy the boundary conditions at $x = \pm s$. The variational problem

$$\delta w = 0 \tag{22}$$

gives

$$-2\int_{-s}^{s}(\mu\Phi'' + \mu'\Phi' - \beta^2\Phi)\delta\Phi\,dx + 2\mu\Phi'\delta\Phi\Big|_{-s}^{s} + \frac{\partial F_1}{\partial\Phi}\delta\Phi\Big|_s + \frac{\partial F_2}{\partial\Phi}\delta\Phi\Big|_{-s} = 0. \tag{23}$$

The integral in (23) vanishes for all the solutions of (13). The functions F_1 and F_2 have now to be determined so that the remaining part of (23) vanishes due to the boundary conditions (14)–(19). That is, F_1 and F_2 must satisfy

$$\left(2\mu\Phi' + \frac{\partial F_1}{\partial\Phi}\right)\Big|_s = 0 \tag{24}$$

and

$$\left(-2\mu\Phi' + \frac{\partial F_2}{\partial\Phi}\right)\Big|_{-s} = 0. \tag{25}$$

In Appendix A, we show that

$$F_1(\Phi)|_s = \beta\tanh(\beta t_1)\Phi^2(s) \tag{26}$$

$$F_2(\Phi)|_{-s} = \beta\tanh(\beta t_2)\Phi^2(-s) \tag{27}$$

where $t_1 = d - s$ and $t_2 = t - s$. The functional w of the variational problem can thus be written

$$w=\mu_0\int_{-s}^{s}\left[\mu(\Phi')^2+\beta^2\Phi^2\right]dx$$
$$+\mu_0\beta\left[\tanh(\beta t_1)\Phi^2(s)+\tanh(\beta t_2)\Phi^2(-s)\right]. \quad (28)$$

We recognize (24) and (25) as the natural boundary conditions of the variational problem which, according to (16) and (17), simply require the continuity of $\bar{b}\cdot\hat{x}$ at the film–dielectric interfaces. (In making this identification, (18) and (19) for the continuity of the potential and (14) and (15) manifesting the existence of the ground planes at $x=-t$ and $x=d$ have also been used.) Further, the Lagrangian (20) is identical with the magnetic quasi-energy density $\bar{b}\cdot\bar{h}^*$, as can be seen by direct use of (11b) and (12b). In the same spirit, using the appropriate parts of (11) and (12) to form the product $\bar{b}\cdot\bar{h}^*$ in the dielectric regions I and III, integrating with respect to x and using the boundary conditions (14)–(19), the expressions

$$\int_s^d\bar{b}\cdot\bar{h}^*\,dx=\beta\tanh(\beta t_1)\Phi^2(s) \quad (29)$$

and

$$\int_{-t}^{-s}\bar{b}\cdot\bar{h}^*\,dx=\beta\tanh(\beta t_2)\Phi^2(-s) \quad (30)$$

can be obtained. The functional (28) can thus be written

$$w=\int_{-t}^{d}\bar{b}\cdot\bar{h}^*\,dx. \quad (31)$$

The physical interpretation of (31) is given in [1].

We now consider the expansion of the potential profile $\Phi(x)$ in a set of functions $\{f_0(x),f_1(x),\cdots\}$ complete in the interval $[-s,s]$

$$\Phi(x)=C_i f_i(x) \quad (32)$$

where the summation is assumed over the repeated indices. Substitution of (32) into (28) yields the quadratic form

$$w=a_{ij}C_iC_j \quad (33)$$

with

$$a_{ij}=\mu_0\beta\left[\tanh(\beta t_2)f_if_j|_{-s}+\tanh(\beta t_1)f_if_j|_s\right]$$
$$+\mu_0\int_{-s}^{s}\left(\mu f_i'f_j'+\beta^2f_if_j\right)dx. \quad (34)$$

To recapitulate, w is stationary for the correct fields; this means, according to (33), that w is stationary for the correct coefficients C_i. (It is well known [3] that, as a quadratic form, w is stationary when the C_i's are the components of the eigenvectors of a_{ij} and the values of w for these C_i's are proportional to the eigenvalues of a_{ij}.)

It can be shown that w vanishes for all correct fields of the magnetostatic problem [1], [2]. Thus, it is only the zero eigenvalue of a_{ij} that will give us the desired solutions. The condition on a_{ij} so that zero is indeed an eigenvalue is

$$\det(a_{ij})=0. \quad (35)$$

Solution of (35) for β gives the wavenumbers of the modes allowed for each frequency. This process is repeated for different frequencies in order to obtain the dispersion relation $\beta=\beta(\omega)$. The delay $\tau=\tau(\omega)$ can be calculated by taking a numerical derivative of the dispersion relation.

IV. FVW Variational Formulation

FVW modes are supported by a bias field $H=H_0\hat{x}$, in which case the internal field H_i is given by

$$H_i=H_0-M_s(x). \quad (36)$$

According to (6) and (11) and using the expression (2) for the permeability tensor, the small-signal $\bar{b}$ field is

$$\bar{b}_{\mathrm{I}}=\mu_0\bar{h}_{\mathrm{I}} \quad (37a)$$
$$\bar{b}_{\mathrm{II}}=-\mu_0\left[\phi'(x)\hat{x}+\kappa\beta\Phi\hat{y}+i\mu\beta\Phi\hat{z}\right]e^{i\beta z} \quad (37b)$$
$$\bar{b}_{\mathrm{III}}=\mu_0\bar{h}_{\mathrm{III}}. \quad (37c)$$

Substituting (37b) into (7), we obtain the equation

$$\Phi''-\mu\beta^2\Phi=0 \quad (38)$$

for the potential profile $\Phi(x)$ inside the ferrimagnet.

Application of the boundary condition (8) on the perfect conductors and the film–dielectric interfaces gives

$$A_1e^{-\beta d}-A_2e^{\beta d}=0 \quad (39)$$
$$D_1e^{\beta t}-D_2e^{-\beta t}=0 \quad (40)$$
$$-\Phi'|_s=\beta\left(A_1e^{-\beta s}-A_2e^{\beta s}\right) \quad (41)$$
$$-\Phi'|_{-s}=\beta\left(D_1e^{\beta s}-D_2e^{-\beta s}\right) \quad (42)$$

while application of condition (9) at the interfaces gives

$$A_1e^{-\beta s}+A_2e^{\beta s}=\Phi(s) \quad (43)$$
$$D_1e^{\beta s}+D_2e^{-\beta s}=\Phi(-s). \quad (44)$$

Proceeding as before, the Lagrangian giving rise to (38) is

$$L=(\Phi')^2+\mu\beta^2\Phi^2 \quad (45)$$

and the functional with natural boundary conditions given by the (39)–(42) is

$$w=\mu_0\int_{-s}^{s}\left[(\Phi')^2+\mu\beta^2\Phi^2\right]dx$$
$$+\mu_0\beta\left[\tanh(\beta t_1)\Phi^2(s)+\tanh(\beta t_2)\Phi^2(-s)\right]. \quad (46)$$

This functional is also a special case of (31). By expanding the potential as in (32), we obtain

$$w=A_{ij}C_iC_j \quad (47)$$

with

$$A_{ij}=\mu_0\beta\left[\tanh(\beta t_2)f_if_j|_{-s}+\tanh(\beta t_1)f_if_j|_s\right]$$
$$+\mu_0\int_{-s}^{s}\left(f_i'f_j'+\mu\beta^2f_if_j\right)dx. \quad (48)$$

Using the same arguments as in Section III, the wavenumbers of the modes propagating at a given frequency are found from the zeros of the equation

$$\det(A_{ij})=0. \quad (49)$$

The dispersion relation of each mode, $\beta=\beta(\omega)$, as well as its delay, are found as in the BVW case.

V. General Properties

In contrast to surface waves, it is well known that magnetostatic volume waves in inhomogeneous films are reciprocal [4], [5]. The effects of inhomogeneities on the reciprocity of volume waves have been examined by Morgenthaler [6], [7] and Stancil [2]. In agreement with the general conditions for reciprocity discussed in [2], we point out that both backward and forward volume waves are reciprocal in our geometry. This property can be seen by noting that the matrix elements a_{ij} and A_{ij} are even functions of the wavenumber β.

For surface MSW's, it has been shown that the quantity βs is invariant under scale transformations provided the magnetization profile is scaled appropriately [1]. In Appendix B, we show that volume MSW's also preserve the quantity βs under the same conditions. Specifically, if we consider the point transformation

$$\tilde{x} = \epsilon x \tag{50}$$

and two film geometries such that

$$\tilde{M}_s(\tilde{x}) = M_s(x) \tag{51}$$

with all the length quantities related by (50), then

$$\beta(\omega) = \epsilon\tilde{\beta}(\omega) \tag{52}$$

and

$$\tau(\omega) = \epsilon\tilde{\tau}(\omega) \tag{53}$$

where $\tilde{\beta}$ and $\tilde{\tau}$ are the wavenumber and the delay, respectively, of an expanded ($|\epsilon| > 1$) or contracted ($|\epsilon| < 1$) film geometry.

For the special case of isolated homogeneous films, it can be shown [4], [5] that volume MSW's propagate in the frequency range

$$\omega_L \leqslant \omega \leqslant \omega_H \tag{54}$$

where

$$\omega_L = -\gamma\mu_0 H_i \tag{55}$$

and

$$\omega_H = -\gamma\mu_0\left[H_i(H_i + M_s)\right]^{1/2}. \tag{56}$$

For each frequency in the above band, there are countably infinite β modes. All of the modes have the same lower and upper frequency cutoffs. Furthermore, for BVW

$$\lim_{\beta \to 0^+} \omega(\beta) = \omega_H \tag{57a}$$

and

$$\lim_{\beta \to \infty} \omega(\beta) = \omega_L \tag{57b}$$

while for FVW

$$\lim_{\beta \to 0^+} \omega(\beta) = \omega_L \tag{58a}$$

and

$$\lim_{\beta \to \infty} \omega(\beta) = \omega_H. \tag{58b}$$

The presence of the ground planes changes the dispersion of a homogeneous film [8]–[12] but does not change the above frequency band edges if $t_1 + t_2 \to \infty$ [13].

With the exception of the lower frequency limit of BVW's, the frequency limits given by (55) and (56) are not fixed if the magnetization profile is nonuniform. Instead, they vary with the magnetization throughout the film thickness. (The low-frequency limit in the BVW geometry remains fixed, however, since the absence of a demagnetizing field makes the internal field independent of M_s.)

Previous work on geometries with several homogeneous ferrimagnetic layers [12], [14] has shown that modes exist that are associated with the magnetization of each layer. Consequently, these modes propagate in different frequency bands according to (54)–(56). These properties are naturally extended to the more general case of an arbitrary thickness variation of the magnetization if, for each particular configuration and $M_s(x)$ profile, we define the frequencies

$$\omega_{L\,\max} = \max \omega_L(x), \qquad x \in [-s, s] \tag{59}$$

and

$$\omega_{H\,\min} = \min \omega_H(x), \qquad x \in [-s, s]. \tag{60}$$

For every magnetization profile we have considered, we have found a class of modes whose $\beta \to 0$ cutoff frequencies are given by (59) for FVW's and (60) for BVW's. In this paper, we present the delay of the lowest β mode with these band edges. The higher order modes with the same frequency cutoffs are not shown due to their long delay. Modes that exist for frequencies outside this frequency passband will be the topic of a future paper.

VI. Numerical Examples

A computer program has been written to calculate the matrices (34) and (48) and their determinants. The dispersion relation, the potential, and the delay characteristics of the waves are obtained as described in Section III. Legendre polynomials defined in the interval $[-s, s]$ have been chosen for the basis functions $f_0, f_1, \cdots$, in our analysis. These functions are convenient because of their orthogonality in the interval $[-s, s]$ and the fast convergence they provide in the case of a homogeneous magnetization film.

As an example of the rapid convergence obtained with Legendre functions, consider an isolated film ($t_1, t_2 \to \infty$) of thickness 30 μm and magnetization $M_s = 140.06$ kA/m ($4\pi M_s = 1760$ G). In this case, the exact solution can be found analytically. For FVW's with a bias field $H_0 = 237.8$ kA/m (3000 Oe), the passband extends from 3.472 to 5.400 GHz (cf. eq. (54)). The wavenumber, calculated by our method using only one term in (32), had a relative error ($|\beta_{\text{exact}} - \beta_{\text{var}}|/\beta_{\text{exact}}$) of 0.291 percent at 3.50 GHz. By using three terms, the error was reduced to 0.093 percent. At 4.50 GHz, and using three terms, the error was 0.010 percent, while with five terms it was reduced to 0.001 percent. For BVW's with a bias field $H_0 = 47.7$ kA/m (600 Oe), the passband extends from 1.680 to 3.332 GHz. The

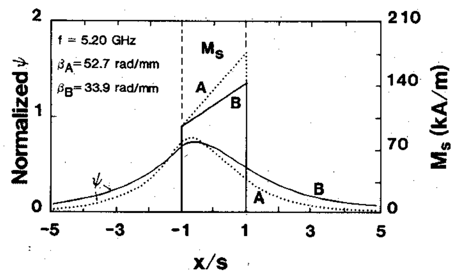

(a)

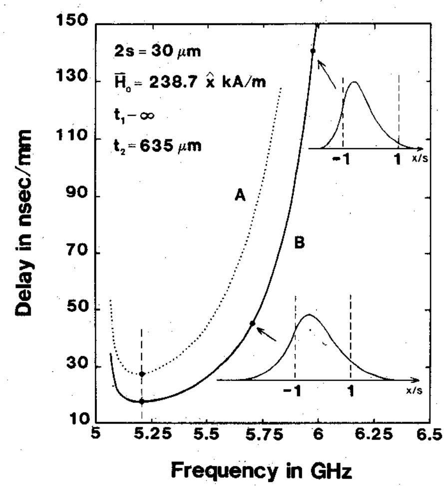

(b)

Fig. 2. FVW propagation. (a) The potentials of two linear profiles (A, B) at $f = 5.20$ GHz. (b) The delay characteristics and additional potential profiles. The vertical dashed line indicates the frequency used for the potential profiles in part (a).

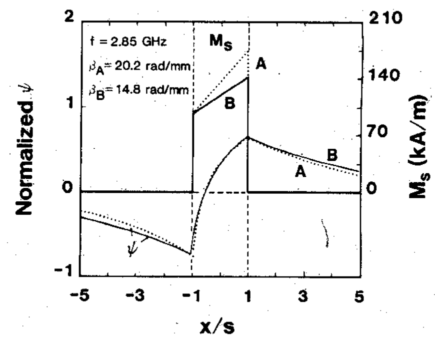

(a)

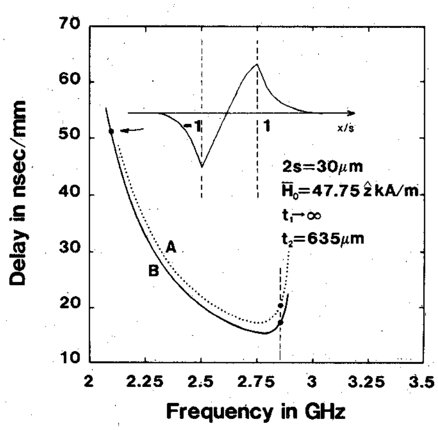

(b)

Fig. 3. BVW propagation. (a) The potentials of two linear profiles (A, B) at $f = 2.85$ GHz. (b) The delay characteristics and additional potential profiles. The vertical dashed line indicates the frequency used for the potential profiles in part (a).

wavenumber, calculated using three terms in (32), was found with an error of 0.00214 percent at 3.30 GHz. By using five terms, the error was reduced to 0.000047 percent.

Two linear magnetization profiles, A and B, and their FVW potentials at 5.20 GHz, are shown in Fig. 2(a). Both of them have the same low M_s value of 95.49 kA/m ($4\pi M_s = 1200$ G). Their average magnetization values are 136.40 kA/m ($4\pi M_s = 1714$ G) and 119.37 kA/m ($4\pi M_s = 1500$ G) for A and B, respectively. The gyromagnetic ratio ($\gamma/2\pi = 28$ GHz/T), layer thickness ($2s = 30$ μm), ground plane distances ($t_1 \rightarrow \infty$, $t_2 = 635$ μm), and the bias field ($H_0 = 238.7$ kA/m (3000 Oe)) are the same for both films. The FVW passband for a film of $M_s = 95.49$ kA/m with the above gyromagnetic ratio and bias field extends from $f_L = 5.040$ GHz to $f_H = 6.507$ GHz. Fig. 2(b) shows the delays of the above films, together with the potential functions of profile B at the frequencies 5.7 GHz and 5.98 GHz. From the delay curves, it is apparent that both films have the same low-frequency cutoff at $f = 5.040$ GHz, which corresponds to that of a uniform film of $M_s = 95.49$ kA/m. If the film were homogeneous, the potential profile of the lowest mode would be an even function of x. For the case of the linearly inhomogeneous film, we see that the potential of the lowest mode in our terminology is neither even nor odd. Instead, it is shifted towards the low-magnetization side of the film. Film A has a higher β than does B for the same frequency; this results in a stronger localization of its potential at a given frequency, as is apparent from Fig. 2(a). This can be qualitatively explained by introducing the notion of an effective film thickness experienced by the mode that decreases as the slope of the magnetization increases. In accordance with this interpretation, the delay of film A is greater than that of film B for a given frequency because of the smaller effective thickness of A.

The same two M_s profiles used above are now considered for BVW propagation. A bias field $H_0 = 47.74$ kA/m (600 Oe) is applied. The BVW passband for the minimum magnetization in the film (95.49 kA/m) extends from 1.680 GHz to 2.910 GHz. Fig. 3(a) shows the M_s profiles and the corresponding potentials for the lowest modes for $f = 2.85$ GHz. The delays for these modes are shown in Fig. 3(b). The upper frequency cutoffs are the same for both films since, as argued earlier, the lowest mode is associated with the minimum M_s in the film, which is the same (95.49 kA/m) for both A and B.

Two magnetization profiles representative of films that have been ion implanted below the level that renders the material paramagnetic [15], [16] are shown in Fig. 4(a). Both films have the same gyromagnetic ratio (28 GHz/T), and a bias field of $H_0 = 238.7$ kA/m (3000 Oe) is applied normal to the slab. The minimum magnetization of film A is 84.03 kA/m ($4\pi M_s = 1056$ G) which is 60 percent of the original magnetization of 140.06 kA/m ($4\pi M_s = 1760$ G).

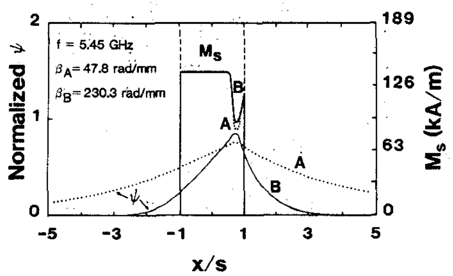

(a)

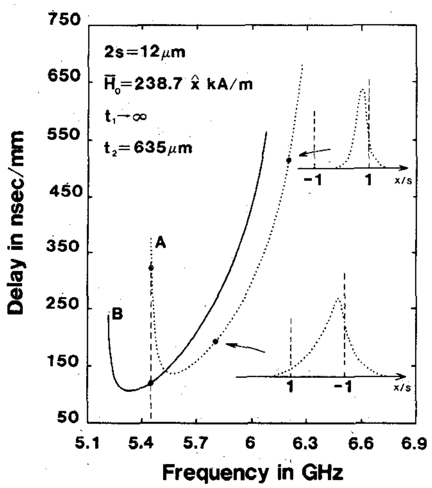

(b)

Fig. 4. FVW propagation. (a) The potential for two ion-implanted films at $f = 5.45$ GHz. (b) The delay characteristics and additional potential profiles. The vertical dashed line indicates the frequency used for the potential profiles in part (a).

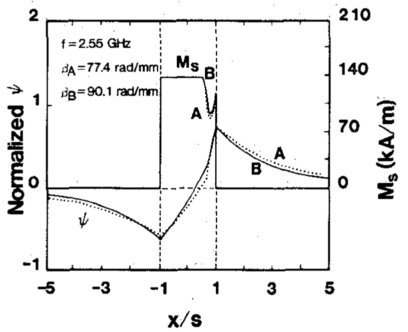

(a)

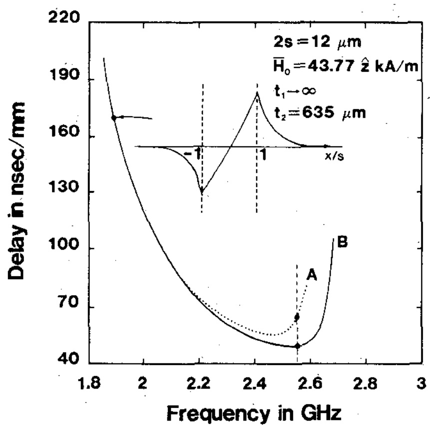

(b)

Fig. 5. BVW propagation. (a) The potential for two ion-implanted films at $f = 2.55$ GHz. (b) The delay characteristics and additional potential profiles. The vertical dashed line indicates the frequency used for the potential profiles in part (a).

The minimum magnetization of film B is 91.04 kA/m ($4\pi M_s = 1144$ G), which is 75 percent of the original M_s. The corresponding FVW low-frequency cutoffs are 5.443 and 5.197 GHz for film A and B, respectively. The difference in the low-frequency cutoffs is illustrated by the delay curves of Fig. 4(b). FVW potential profiles are also shown for film A at 5.8 and 6.2 GHz. The association of the mode with the minimum magnetization value of the film is clearly shown by these profiles.

The same two ion-implanted profiles used above are now considered for BVW propagation. An in-plane field $H_0 =$ 43.77 kA/m (550 Oe) is applied. Fig. 5(a) shows the M_s profiles and the corresponding potentials for $f = 2.55$ GHz. The upper frequency cutoffs are 2.632 GHz and 2.703 GHz for films A and B, respectively. This difference in the upper frequency cutoffs is illustrated by the delay curves of Fig. 5(b).

Ten terms have been used in the expansion of the potential for all the linear profile cases presented above. Fifteen and thirty-five terms have been kept for the ion-implanted films in the forward and backward volume-wave case, respectively. For inhomogeneous M_s, the exact wavenumber is not available. In this case, the convergence of β is tested by a modified Cauchy criterion. If β_n stands for the wavenumber found by (35) or (49) using n terms in the expansion (32), then convergence is obtained by requiring the quantity $\zeta_n = |\beta_{n+1} - \beta_n|/\beta_n$ to be sufficiently small.

TABLE I
FORWARD VOLUME-WAVE CONVERGENCE DATA

Film (Fig.-Profile)	n (No. terms)	$\zeta_n/10^{-5}$	Frequency (GHz)
2-A	10	3.668	5.05
2-A	10	1.102	5.10
2-B	10	1.553	5.05
2-B	10	0.015	6.10
4-A	15	0.199	5.45
4-A	15	1.512	6.20
4-B	15	19.82	5.25
4-B	15	2.436	5.90

Numerically, this quantity has been found to be frequency-dependent. Convergence data for the profiles presented in Figs. 2–5 are summarized in Tables I and II.

It should be mentioned that the modes presented here have not been considered in previous work on MSW propagation in ion-implanted films [17], [18]. The $\beta \to 0$ FVW-mode cutoffs for the modes in these previous studies are obtained using the value of the unperturbed magnetization rather than the minimum magnetization. Thus, the FVW modes discussed here propagate at higher frequencies and longer delays than the modes associated with the unperturbed region. These new modes may contribute sig-

TABLE II
BACKWARD VOLUME-WAVE CONVERGENCE DATA

Film (Fig.-Profile)	n (No. terms)	$\zeta_n/10^{-5}$	Frequency (GHz)
3-A	10	5.021	2.85
3-A	10	652.7	2.90
3-B	10	0.309	2.85
3-B	10	269.1	2.90
5-A	35	0.037	1.90
5-A	35	1.389	2.55
5-B	35	0.007	1.90
5-B	35	1.548	2.63

nificantly to an increased insertion loss of ion-implanted devices. Also in these previous studies, doses beyond the level that destroys ferrimagnetism and multiple ion implantations were employed to obtain profiles that could be approximated by uniform layers. With the present variational formulation, however, arbitrary single or multiple implantation profiles can be analyzed.

VII. SUMMARY

Magnetization inhomogeneities in ferrite film geometries have been used to control dispersion, form array reflectors, and occur naturally at the film–substrate interface. We have presented a method for analyzing magnetostatic volume-wave modes in thin films with arbitrary variations of M_s through the thickness. Our discussion has been limited to the lowest order modes associated with the minimum magnetization.

APPENDIX A

Equations (14) and (18) can be solved for A_1 and A_2 giving

$$A_1 = \frac{\Phi(s)e^{\beta d}}{2\cosh(\beta t_1)} \tag{A1}$$

and

$$A_2 = \frac{\Phi(s)e^{-\beta d}}{2\cosh(\beta t_1)} \tag{A2}$$

where $t_1 = d - s$. Using (A1) and (A2) in (16), we have

$$-\mu\Phi'|_s = \beta\frac{\Phi(s)}{2\cosh(\beta t_1)}\left[e^{\beta(d-s)} - e^{-\beta(d-s)}\right]$$
$$= \beta\tanh(\beta t_1)\Phi(s). \tag{A3}$$

Substituting (A3) into (24) gives

$$F_1(\Phi)|_s = \beta\tanh(\beta t_1)\Phi^2(s). \tag{A4}$$

Similarly

$$F_2(\Phi)|_{-s} = \beta\tanh(\beta t_2)\Phi^2(-s) \tag{A5}$$

where $t_2 = t - s$.

APPENDIX B

Consider a geometry related to that of Fig. 1 by a change of scale according to the point transformation

$$\tilde{x} = \epsilon x \tag{B1}$$

where quantities in the transformed system are indicated by a tilde. The potential transforms as a scalar

$$\tilde{\Phi}(\tilde{x}) = \Phi(x) \tag{B2}$$

while its derivative transforms as

$$\tilde{\Phi}'(\tilde{x}) = \frac{1}{\epsilon}\Phi'(x). \tag{B3}$$

If the magnetization profile is also scaled so that

$$\tilde{M}_s(\tilde{x}) = M_s(x) \tag{B4}$$

then

$$\tilde{\mu}(\tilde{x}) = \mu(x). \tag{B5}$$

The variational problem for BVW in the transformed system reads

$$\tilde{w} = 0 \tag{B6}$$

$$\delta\tilde{w} = 0 \tag{B7}$$

where

$$\tilde{w} = \mu_0\int_{-\tilde{s}}^{\tilde{s}}\left[\tilde{\mu}(\tilde{\Phi}')^2 + \tilde{\beta}^2\tilde{\Phi}^2\right]d\tilde{x} + \mu_0\tilde{\beta}\left[\tanh(\tilde{\beta}\tilde{t}_1)\tilde{\Phi}^2(\tilde{s}) + \tanh(\tilde{\beta}\tilde{t}_2)\tilde{\Phi}^2(-\tilde{s})\right]. \tag{B8}$$

Substituting (B2), (B3), and (B5) into (B8), $\tilde{w}$ can be rewritten as

$$\tilde{w} = \mu_0\int_{-s}^{s}\left[\frac{\mu}{\epsilon^2}(\Phi')^2 + \frac{\tilde{\beta}^2\epsilon^2}{\epsilon^2}\Phi^2\right]\epsilon\,dx + \mu_0\frac{\tilde{\beta}\epsilon}{\epsilon}\left[\tanh(\tilde{\beta}\epsilon t_1)\Phi^2(s) + \tanh(\tilde{\beta}\epsilon t_2)\Phi^2(-s)\right] \tag{B9}$$

or

$$\epsilon\tilde{w} = \mu_0\int_{-s}^{s}\left[\mu(\Phi')^2 + (\tilde{\beta}\epsilon)^2\Phi^2\right]dx + \mu_0\tilde{\beta}\epsilon\left[\tanh(\tilde{\beta}\epsilon t_1)\Phi^2(s) + \tanh(\tilde{\beta}\epsilon t_2)\Phi^2(-s)\right] \tag{B10}$$

which, by comparison with (28), has wavenumber solutions of the form

$$\beta = \epsilon\tilde{\beta}. \tag{B11}$$

Similarly, the above can be proved to be a property of the FVW as well. By taking the derivative of (B11) with respect to ω the corresponding relation for the delays is found to be

$$\tau(\omega) = \epsilon\tilde{\tau}(\omega). \tag{B12}$$

REFERENCES

[1] N. E. Buris and D. D. Stancil, "Magnetostatic surface wave propagation in ferrite thin films with arbitrary variations of the magnetization through the film thickness," *IEEE Trans. Microwave Theory Tech.*, vol. MTT-33, p. 485, June 1985.

[2] D. D. Stancil, "Variational formulation of magnetostatic wave dispersion relations," *IEEE Trans. Magn.*, vol. MAG-19, p. 1865, 1983.

[3] C. Caratheodory, *Calculus of Variations and Partial Differential Equations of the First Order.* New York: Chelsea Publishing, 1982, p. 177.

[4] R. W. Damon and J. R. Eshbach, "Magnetostatic modes of a ferromagnet slab," *J. Phys. Chem. Solids*, vol. 19, p. 308, 1961.

[5] R. W. Damon and H. Van De Vaart, "Propagation of magnetostatic spin waves at microwave frequencies in normally-magnetized disk," *J. Appl. Phys.*, vol. 36, p. 3453, 1965.

[6] F. R. Morgenthaler, "Nondispersive magnetostatic forward volume waves under field gradient control," *J. Appl. Phys.*, vol. 53, p. 2652, 1982.

[7] F. R. Morgenthaler, "Control of magnetostatic waves in thin films by means of spatially nonuniform bias fields," *Circuits Systems Signal Process.*, vol. 4, nos. 1–2, 1984.

[8] W. L. Bongianni, "Magnetostatic propagation in a dielectric layered structure," *J. Appl. Phys.*, vol. 43, p. 2541, 1972.

[9] M. C. Tsai, H. J. Wu, J. M. Owens, and C. V. Smith, Jr., "Magnetostatic propagation for uniform normally-magnetized multilayer planar structures," *AIP Conf. Proc.*, vol. 34, p. 280, 1976.

[10] M. R. Daniel and P. R. Emtage, "Magnetostatic volume wave propagation in a ferrimagnetic double layer," *J. Appl. Phys.*, vol. 53, p. 3723, 1982.

[11] L. R. Adkins and H. L. Glass, "Magnetostatic volume wave propagation in multiple ferrite layers," *J. Appl. Phys.*, vol. 53, p. 8926, 1982.

[12] P. R. Emtage and M. R. Daniel, "Magnetostatic waves and spin-waves in layered ferrite structures," *Phy. Rev. B*, vol. 29, p. 212, 1984.

[13] T. Yukawa, J. Ikenoue, J. Yamada, and K. Abe, "Effects of metal on dispersion relations of magnetostatic volume waves," *J. Appl. Phys.*, vol. 49, p. 376, 1978.

[14] L. R. Adkins and H. L. Glass, "Propagation of magnetostatic surface waves in multiple magnetic layer structures," *Electron. Lett.*, vol. 16, p. 590, July 17, 1980.

[15] C. H. Wilts and S. Prasad, "Determination of magnetic profiles in implanted garnets using ferromagnetic resonance," *IEEE Trans. Magn.*, vol. MAG-17, p. 2405, 1981.

[16] V. S. Speriosu and C. H. Wilts, "*X*-ray rocking curve and ferromagnetic resonance investigations of ion-implanted magnetic garnet," *J. Appl. Phys.*, vol. 54 (6), p. 3325, June 1983.

[17] P. Hartemann and D. Fontaine, "Influence of ion implantation on magnetostatic volume wave propagation," *IEEE Trans. Magn.*, vol. MAG-18, p. 1595, 1982.

[18] D. Fontaine and P. Hartemann, "Harmonic level reduction in arrays reflecting magnetostatic forward volume waves," *IEEE Trans. Magn.*, vol. MAG-20, p. 1241, 1984.

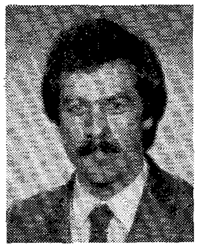

Nikolaos E. Buris (S'84) was born in Karistos, Greece, on May 14, 1958. He received the diploma of electrical engineering from the National Technical University of Athens (E.M.Π.), Greece, in 1982, where his thesis work was on the scattering of electromagnetic waves from cylindrical objects. He is currently working toward his Ph.D. in the ECE Department of North Carolina State University. His current interests are in mathematical methods of physics.

Mr. Buris is a member of the Technical Chamber of Greece.

Daniel D. Stancil (S'80–M'81) was born in Raleigh, NC, in 1954. He received the B.Sc. degree in electrical engineering from Tennessee Technological University in 1976, and the S.M., E.E., and Ph.D. degrees from the Massachusetts Institute of Technology in 1978, 1979, and 1981, respectively.

Since 1981, he has been an Assistant Professor of Electrical Engineering at North Carolina State University, Raleigh, NC. His research and teaching activities have focused on magnetostatic waves in thin ferrite films, electromagnetic waves, and the physics of magnetism.

Dr. Stancil is a member of the American Association for the Advancement of Science, and of the Sigma Xi, Phi Kappa Phi, Tau Beta Pi, and Eta Kappa Nu honorary professional societies.